Spatiotemporal expression patterns of sialoglycoconjugates during nephron morphogenesis and their regional and cell type-specific distribution in adult rat kidney

Zuber, Christian ; Winter, Harry C ; Goldstein, Irwin J ; et al

Abstract: The expression of 2,6- and 2,3-linked sialic acids on N-glycans was studied in embryonic, postnatal, and adult rat kidney. Histochemistry and blotting using Polyporus squamosus and Sambucus nigra lectins for 2,6-linked sialic acids and the Maackia amurensis lectin for 2,3-linked sialic acids were performed and sialyltransferase activity was assayed. N-glycans with 2,6- and 2,3-linked sialic acid were differently expressed in the two embryonic anlagen and early stages of nephron. Metanephrogenic mesenchyme was positive for 2,3-linked sialic acid but not for the 2,6-linked one, which became detectable initially in the proximal part of S-shaped bodies. Collecting ducts were positive for 2,6-linked sialic acid, whereas 2,3-linked sialic acid was restricted to their ampullae. Although positive in embryonic kidney, S1 and S2 of proximal tubules became unreactive for 2,3-linked sialic acid in postnatal and adult kidneys. In adult kidney, intercalated but not principal cells of collecting ducts were reactive for 2,3-linked sialic acid. In contrast, 2,6-linked sialic acids were detected in all cells of adult kidney nephron. Blot analysis revealed a different but steady pattern of bands reactive for 2,6- and 2,3-linked sialic acid in embryonic, postnatal, and adult kidney. Activity of 2,6 and 2,3 sialyltransferases was highest in embryonic kidney and decreased over postnatal to adult kidney with the activity of 2,6 sialyltransferase always being three to fourfold that of 2,3 sialyltransferase. Thus, 2,6- and 2,3-linked sialic acids are differently expressed in embryonic anlagen and mesenchyme-derived early stages of nephron and show regional and cell type-specific differences in adult kidney

DOI: https://doi.org/10.1007/s00418-003-0553-0

Histochem Cell Biol (2003) 120:143–160
DOI 10.1007/s00418-003-0553-0

ORIGINAL PAPER

Christian Zuber · James C. Paulson · Valeriu Toma · Harry C. Winter · Irwin J. Goldstein · Jürgen Roth

Spatiotemporal expression patterns of sialoglycoconjugates during nephron morphogenesis and their regional and cell type-specific distribution in adult rat kidney

Accepted: 27 June 2003 / Published online: 26 July 2003

Abstract The expression of α2,6- and α2,3-linked sialic acids on *N*-glycans was studied in embryonic, postnatal, and adult rat kidney. Histochemistry and blotting using *Polyporus squamosus* and *Sambucus nigra* lectins for α2,6-linked sialic acids and the *Maackia amurensis* lectin for α2,3-linked sialic acids were performed and sialyltransferase activity was assayed. *N*-glycans with α2,6- and α2,3-linked sialic acid were differently expressed in the two embryonic anlagen and early stages of nephron. Metanephrogenic mesenchyme was positive for α2,3-linked sialic acid but not for the α2,6-linked one, which became detectable initially in the proximal part of S-shaped bodies. Collecting ducts were positive for α2,6-linked sialic acid, whereas α2,3-linked sialic acid was restricted to their ampullae. Although positive in embryonic kidney, S1 and S2 of proximal tubules became unreactive for α2,3-linked sialic acid in postnatal and adult kidneys. In adult kidney, intercalated but not principal cells of collecting ducts were reactive for α2,3-linked sialic acid. In contrast, α2,6-linked sialic acids were detected in all cells of adult kidney nephron. Blot analysis revealed a different but steady pattern of bands reactive for α2,6- and α2,3-linked sialic acid in embryonic, postnatal, and adult kidney. Activity of α2,6 and α2,3 sialyltransferases was highest in embryonic kidney and decreased over postnatal to adult kidney with the activity of α2,6 sialyltransferase always being three to fourfold that of α2,3 sialyltransferase. Thus, α2,6- and α2,3-linked sialic acids are differently expressed in embryonic anlagen and mesenchyme-derived early stages of nephron and show regional and cell type-specific differences in adult kidney.

Keywords Kidney · Kidney development · Sialic acid · Sialyltransferase · Histochemistry · *Polyporus squamosus* lectin · *Maackia amurensis* lectin

C. Zuber · V. Toma · J. Roth (✉)
Division of Cell and Molecular Pathology,
Department of Pathology,
University of Zürich,
Schmelzbergstrasse 12, 8091 Zürich, Switzerland
e-mail: juergen.roth@usz.ch
Tel.: +41-1-2555090
Fax: +41-1-2554407

J. C. Paulson
The Scripps Research Institute,
Department of Molecular Biology,
La Jolla, CA 92037, USA

H. C. Winter · I. J. Goldstein
Department of Biological Chemistry, School of Medicine,
University of Michigan,
Ann Arbor, Michigan, 48109-0606, USA

Introduction

The kidney belongs to the organs with an exceptional degree of complexity in terms of both morphological organization and function. With regard to the former, three different regions, the cortex and the outer and the inner medulla, can be distinguished because of the presence of different parts of the nephron (Kaissling and Dorup 1995; Kriz and Kaissling 2000). Along the nephron, various cell types can be distinguished fulfilling specific functions in filtering, reabsorption and secretion (Al-Awqati 1996, 2003; Kriz and Kaissling 2000; Pavenstädt et al. 2003). Thus, adult kidney has been subjected to studies on cell type-specific and plasma membrane domain-related expression of *N*- and *O*-glycans present in glycoproteins. For instance, specific expression patterns of sialic acid residues as detected with the *Limax flavus* lectin and of *N*-acetylgalactosamine-terminated oligosaccharides reactive with the *Helix pomatia* lectin were found in the podocyte plasma membrane (Charest and Roth 1985; Roth et al. 1983). Sialoglycoproteins such as podocalyxin and podoplanin have been shown to be involved in establishing and maintaining the peculiar shape of podocytes (Kerjaschki et al. 1984; Matsui et al. 1999; Pavenstädt et al. 2003). Histochemical lectin-binding studies have also revealed a

remarkable degree of variability in glycocalyx composition of the various epithelia present in the distal and collecting tubules (Brown et al. 1985; Kaneko et al. 1995; LeHir and Dubach 1982; LeHir et al. 1982; Roth and Taatjes 1985; Taatjes et al. 1988; Toma et al. 1999), although the functional importance of these differences remains unknown.

The permanent kidney, in contrast to other organs, develops from two different embryonic anlagen, the metanephrogenic mesenchyme and the epithelial ureteric bud, by interactive processes inducing morphogenesis and differentiation (Horster et al. 1999; Saxén 1987). The blind ends of the sprouting and dichotomously branching ureteric bud induce clustering and condensation of the mesenchymal cells. Through growth and differentiation, they initially form the renal vesicle, which is the first epithelial structure and which further differentiates through the S-shaped body and capillary loop stage into maturing glomeruli. This is accompanied by segmental morphogenesis resulting in the formation of proximal and distal tubules with the loop of Henlé in between, and connecting tubules. Thus, the entire epithelium of the nephron is derived from mesenchyme which undergoes a transition into epithelium, whereas the collecting duct system is primarily epithelia-derived. A variety of studies related to the inductive and morphogenetic events during nephrogenesis revealed spatiotemporal expression patterns of cell adhesion molecules, extracellular matrix components, growth factors, transcription factors, and proto-oncogene encoded receptor tyrosine kinases (Bard et al. 1994; Birchmeier and Birchmeier 1993; Hammerman et al. 1992; Horster et al. 1999; Kumar et al. 1997; Parr and McMahon 1994; Rauscher 1993). Spatiotemporal patterns of lectin-binding sites and of polysialic acids have been observed during the formation and differentiation of the nephron (Holthöfer and Virtanen 1987; Kunz et al. 1984; Lackie et al. 1990; Laitinen et al. 1987; Roth et al. 1987; Toma et al. 2000; Wagner and Roth 1988; Ziak and Roth 1999). The studies on polysialic acids disclosed remarkable correlations between their expression and particular stages of nephron development (Lackie et al. 1990; Roth et al. 1987; Ziak and Roth 1999), which were not as obvious for sialoglycoconjugates terminated by a single sialic acid residue as detected with the *Limax flavus* lectin (Wagner and Roth 1988), *Sambucus nigra* lectin, or *Maackia amurensis* lectin (Sata et al. 1989) and Amaranthin (Toma et al. 2000).

The present study was conducted to analyze the presence and distribution of *N*-glycans terminated in sialic acid either in α2,6- or in α2,3-linkage to galactose β1,4 *N*-acetylglucosamine during embryonic development and postnatal differentiation of rat kidney and in the adult organ. For this purpose, the *Polyporus squamosus* lectin, highly reactive with the NeuAcα2,6Galβ1,4GlcNAc trisaccharide sequence (Mo et al. 2000; Zhang et al. 2001), the *Sambucus nigra* lectin reactive with the NeuAcα2,6Gal/GalNAc disaccharide sequence (Shibuya et al. 1987), and the *Maackia amurensis* lectin reactive with the NeuAcα2,3Galβ1,4GlcNAc trisaccharide sequence (Knibbs et al. 1991; Wang and Cummings 1988) were used for histochemistry and blot analysis. Furthermore, the specific activity of the respective sialyltransferases, β-galactoside α2,6 sialyltransferase (ST6Gal-I) and β-galactoside α2,3 sialyltransferase (ST3Gal-III), was determined in tissue extracts. Although sialic acid linked α2,6 or α2,3 to penultimate galactose of oligosaccharides is commonly found in various organs including the kidney (Kelm and Schauer 1997; Paulson and Colley 1989; Rosenberg 1995), our results show hitherto unrecognized differences in their cellular and regional expression during embryonic development and postnatal kidney differentiation and in the adult rat kidney.

Materials and methods

Reagents

Polyporus squamosus lectin (PSL) was affinity purified as described (Mo et al. 2000). Lectin–digoxigenin conjugates were prepared in the presence of 0.2 M galactose and 0.1% Triton X-100 using a digoxigenin conjugation kit from Roche Molecular Biochemicals (Mannheim, Germany) according to the manufacturer's instructions. Digoxigenin conjugates of *Sambucus nigra* lectin (SNL) and *Maackia amurensis* lectin (MAL) were available from previous studies. Horseradish peroxidase or alkaline phosphatase-conjugated sheep anti-digoxigenin antibodies (Fab fragments), neuraminidase from *Vibrio cholerae*, and *N*-glycanase F were from Roche Molecular Biochemicals, and a 4 nm gold-labeled rabbit anti-horseradish peroxidase antibody was from Immunoresearch Laboratories (West Grove, PA). All other reagents were of analytical grade.

Tissue preparation

Sprague-Dawley rats and pregnant rats were obtained from the Central Animal Facility of the University of Zurich. Kidneys from adult rats were fixed by perfusion from the left cardiac ventricle with freshly prepared 3% formaldehyde–0.1% glutaraldehyde or 4% formaldehyde in Hank's balanced salt solution (pH 7.4, 37°C) for 15 min, followed by immersion fixation at ambient temperature for 1 h 45 min. Kidneys from embryonic day 16, 18, and 20 as well as kidney slices from postnatal days 2, 5, 7, 14, and 21 were fixed by immersion in the above fixatives. Free aldehyde groups were blocked by immersing the tissues in 50 mM NH_4Cl in PBS (10 mM phosphate buffer, 0.15 M NaCl, pH 7.4) for 1 h.

Formaldehyde-fixed tissues were embedded in paraffin according to standard protocol and sections of approximately 5 μm thickness were prepared. Large pieces from formaldehyde/glutaraldehyde-fixed adult kidney were embedded at progressively lowered temperature (–42°C finally) in Lowicryl K4 M and used to prepare large 0.5–1.0 μm semithin sections containing cortex and adjacent outer medulla or inner medulla with adjacent outer medulla. Small pieces from kidney cortex and inner medulla were embedded in Lowicryl K4 M for the preparation of ultrathin sections (Roth 1989).

Lectin histochemistry

For light microscopy, a three-step labeling protocol followed by photochemical silver amplification was performed as described in detail previously (Roth et al. 1998; Toma et al. 2001). In brief, deparaffinized and rehydrated paraffin sections or semithin sections of Lowicryl K4 M-embedded tissue were incubated with digoxigenin-conjugated PSL (1.5 μg/ml), SNL (1.25 μg/ml), or MAL

(2.5 μg/ml) in PBS (pH 7.4) containing 1% BSA, 0.05% Tween 20, and 0.005% Triton X-100 for 2 h at ambient temperature, rinsed in buffer, and incubated with horseradish peroxidase-conjugated sheep anti-digoxigenin Fab (0.3 U/ml) for 1 h. After rinses with buffer, sections were incubated with 4 nm gold-labeled anti-horseradish peroxidase antibody (Roth et al. 1992) adjusted to an absorbance of 0.05 at 525 nm. Finally, silver intensification using silver acetate (Roth et al. 1998) was performed followed by counterstaining with nuclear fast red (paraffin sections). Both paraffin and Lowicryl K4 M semithin sections were also incubated with directly gold-labeled SNL and MAL followed by silver intensification of the lectin–gold labeling (Sata et al. 1989).

For electron microscopy, ultrathin sections were incubated with directly gold-labeled MAL (Sata et al. 1989) or with digoxigenin-conjugated MAL followed by 8 nm gold-labeled anti-digoxigenin antibody (Sata et al. 1990).

The specificity of staining was established by incubating the lectins with varying amounts (0.1 mM to 0.2 M) of either 6′ or 3′ sialyllactose for 30 min prior to use to stain paraffin sections from kidney.

Furthermore, specificity of lectin staining was corroborated by enzymatic removal of oligosaccharide side chains at the asparagine-*N*-acetylglucosamine core linkage. For this, paraffin sections were treated with 0.1% sodium dodecyl sulfate in TRIS-buffered saline at 70°C for 30 min and washed in NP40 in TRIS-buffered saline. This was followed by *N*-glycanase F (80 U/ml in 0.1 M phosphate buffer, pH 7.4) in a moist chamber for 18 h at 37°C. Afterwards, tissue sections were conditioned with PBS containing 1% BSA, 0.05% Triton X-100, and 0.05% Tween 20 for 20 min at ambient temperature and incubated with the lectins as described above. To enzymatically remove sialic acids, paraffin sections were treated with *Vibrio cholerae* neuraminidase (0.02 U/ml in 50 mM acetate buffer, pH 5.5) for 18 h at 37°C in a moist chamber, washed, conditioned, and incubated with the lectins as described above. To assess the effect of the incubation buffers on the lectin staining, sections were incubated in the respective enzyme buffers only for 18 h at 37°C before lectin labeling.

Mild base treatment to de-*O*-acetylate sialic acids was performed by treating paraffin sections either with 0.5% KOH in 70% ethanol or with 0.1 N NaOH for 20 min at ambient temperature (Reid et al. 1978).

Sodium dodecyl sulfate-polyacrylamide gel electrophoresis and lectin blotting

Kidneys from embryonic day 20, postnatal days 2, 5, 7, 14, and 21 as well as adult animals were homogenized in PBS (pH 7.4) containing protease inhibitor tablets, and proteins were extracted with 1% Triton X-100 for 1 h at 4°C. Extracts were also prepared from microscopically dissected kidney cortex and inner medulla. The homogenates were centrifuged at 14,000 *g* for 10 min at 4°C and aliquots of the supernatants were used for SDS-PAGE. Lectin blotting was performed as described in detail previously (Zuber et al. 1998). In brief, proteins were denatured in Laemmli buffer and then separated by 3–15% gradient SDS-PAGE (100 μg/lane) and transferred to nitrocellulose membranes. Nitrocellulose membranes were incubated with digoxigenin-conjugated PSL (2.5 μg/ml PBS containing 0.05% Tween 20 and 1% BSA) or MAL (5 μg/ml 0.1 M TRIS-HCl, pH 7.5, 0.15 M NaCl containing 0.05% Tween 20 and 1% BSA) for 2 h, washed, and incubated with alkaline phosphatase-conjugated anti-digoxigenin antibody (0.25 U/ml TRIS-buffered saline containing Tween 20) for 45 min followed by color reaction.

Sialyltransferase assays

Homogenates from whole kidneys from embryonic day 20, postnatal days 2, 5, 7, 14, and 21 as well as adult whole kidneys were assayed. Furthermore, homogenates from kidney cortex, outer and inner medulla obtained by microscopic dissection were assayed. The activity of the β-galactoside α2,6 sialyltransferase (ST6Gal-I) and β-galactoside α2,3 sialyltransferase (ST3Gal-III) was assessed in identical reaction mixtures with the exception of their specific acceptor substrates which were asialo-α_1-acid glycoprotein and lacto-*N*-tetraose as described in detail previously (Weinstein et al. 1982).

Results

Distribution pattern of α2,6- and α2,3-linked sialic acid in embryonic kidneys

Staining for both PSL and MAL indicative of the presence of oligosaccharides terminated in α2,6- and α2,3-linked sialic acid, respectively, was detectable in kidneys from embryonic days 16, 18, and 20. In general, the intensity of staining obtained with PSL was lower than that observed with MAL (Figs. 1, 2, 3). Staining patterns for SNL and PSL were identical irrespective of the used techniques. Although PSL staining was observed in all parts of the ureteric bud-derived collecting ducts (*arrows* in Figs. 1B, 2B, 3B), the staining with MAL was restricted to the terminal ampullae of the collecting ducts (*arrows* in Figs. 1D, 2E, 3D). This differential staining pattern was consistently observed in kidneys from embryonic days 16, 18, and 20. The condensed metanephrogenic mesenchyme and the loose mesenchymal stroma were largely unreactive with PSL (Figs. 1B *asterisk*, 2B *asterisk*, 3B). This was in striking contrast to the intense staining observed with MAL in the metanephrogenic mesenchyme of kidneys from embryonic days 16, 18, and 20 (Figs. 1C, D *asterisk*, 2D, E *asterisk*, 3C, D). Additional differences became obvious when the different developmental stages of the glomerulus were considered. Renal vesicles were unreactive with PSL in all embryonic stage kidneys examined (*arrowhead* in Fig. 1B), whereas strong reactivity with MAL was evident in the luminal cell surface and to a lesser degree in the basolateral cell surface of the vesicle epithelia (*arrowhead* in Fig. 1D). The S-shaped bodies showed some PSL reactivity which, however, was restricted to the cells of its proximal part facing the presumptive Bowman's space (*double arrowheads* in Figs. 1B, 2B). In contrast, the entire S-shaped body was stained with MAL (*double arrowheads* in Figs. 1D, 2E, 3D) and the weak staining observed at embryonic day 16 became strong in kidneys from embryonic days 18 and 20. Immature glomeruli which were observed in kidneys from embryonic days 18 and 20 were reactive with both PSL and MAL, in particular the presumptive podocytes (*Gl* in Figs. 2, 3). Likewise, immature proximal tubules observed in kidneys of these embryonic stages were positive for both lectins (Figs. 2C, F *arrows*, 3D *open arrows*). Endothelia of capillaries in the interstitium were faintly positive with PSL (*En* in Fig. 1B) and strongly stained with MAL (*En* in Fig. 1D). This difference in staining intensity was also observed in kidneys from embryonic days 18 and 20 (Figs. 2, 3).

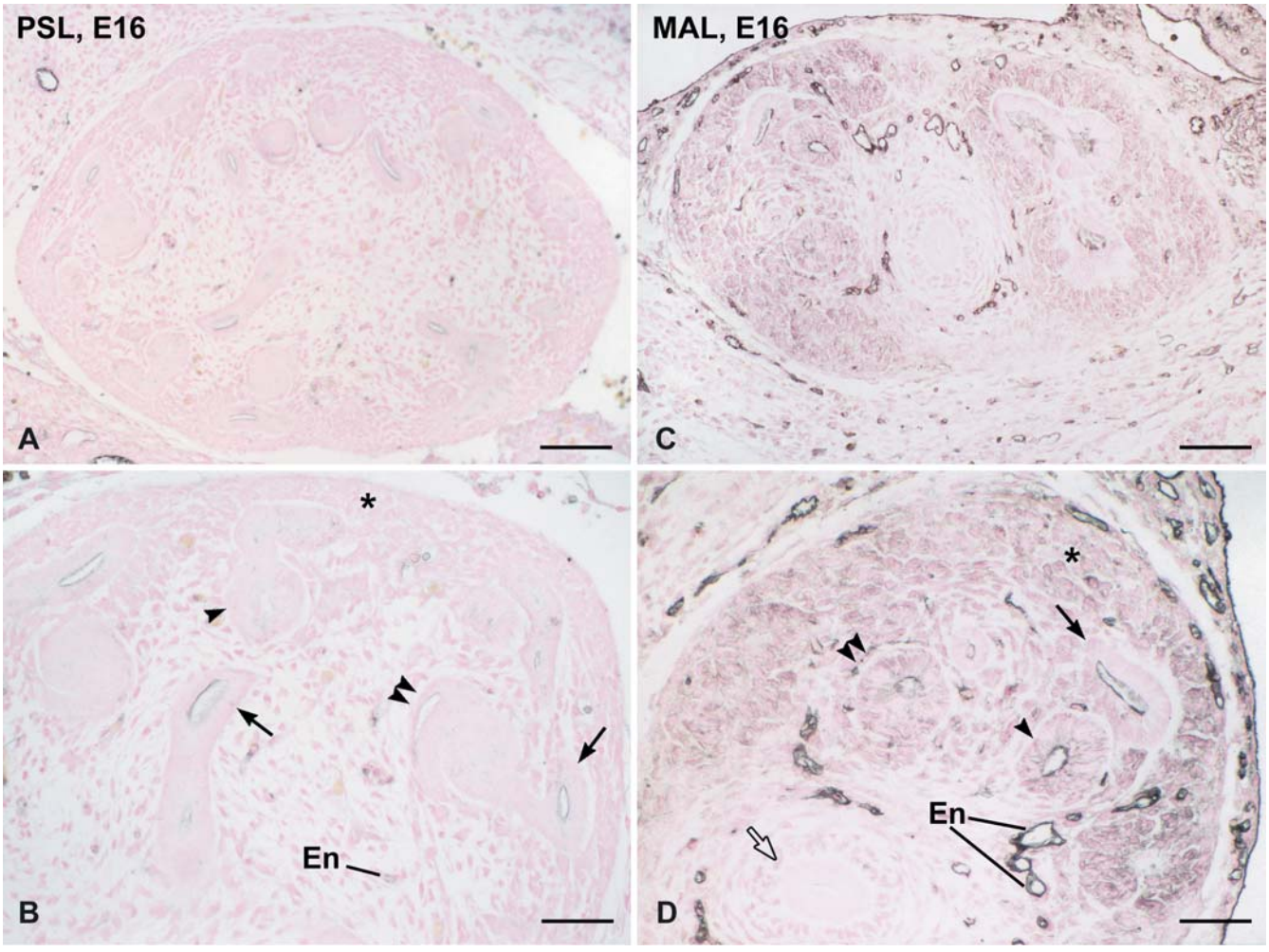

Fig. 1A–D Adjacent sagittal sections of paraffin-embedded rat kidney, embryonic day 16. Silver-intensified lectin–gold staining in this and all other light microscopic illustrations appears in *black*. **A**, **B** Staining with *Polyporus squamosus* lectin (PSL) to detect α2,6-linked sialic acid is observed in ureteric bud-derived collecting ducts and their terminal ampulla (*arrows*). The condensed metanephrogenic mesenchyme (*asterisk*), stromal mesenchyme, and renal vesicle (*arrowhead*) appear unreactive, whereas the crevice of the proximal part of an S-shaped body, which is the first morphological sign of glomerulus formation, is stained (*double arrowheads*). **C**, **D** Staining with *Maackia amurensis* lectin (MAL) to detect α2,3-linked sialic acid. Of the ureteric bud-derived collecting ducts, only the terminal ampulla is stained (*arrow*). The condensed metanephrogenic mesenchyme (*asterisk*), stromal mesenchyme, renal vesicle (*arrowhead*), and entire S-shaped body (*double arrowhead*) are labeled. Both PSL and MAL stain endothelia (*En* in **B** and **D**). *Bars* 90 μm in **A**, **B**; 60 μm in **C**, **D**

In order to exclude that the differences in staining intensity and in distribution pattern were due to *O*-acetylation of sialic acids, tissue sections were subjected to saponification prior to lectin staining. However, no change in intensity and pattern of lectin staining could be observed indicating that the observed differences were not related to *O*-acetylation (not shown).

Distribution pattern of α2,6- and α2,3-linked sialic acid in postnatal kidneys

In rat kidney, nephrogenesis continues in the nephrogenic zone until postnatal day 5. We investigated kidneys from postnatal days 2, 5, 7, 14, and 21. The intensity of PSL staining in postnatal kidneys was stronger than that observed in kidneys from embryonic day 20 with the exception of the nephrogenic zone. At postnatal days 2 (Fig. 4A, B) and 5 (data not shown), the pattern of PSL staining corresponded to the one observed in embryonic day 20 kidneys. Likewise, the MAL staining in the nephrogenic zone was identical to that observed in embryonic kidneys (Fig. 4D). In the underlying cortical region, immature and mature glomeruli were intensely reactive with both PSL (*Gl* in Fig. 4B, see also E) and MAL (*Gl* in Fig. 4D, see also F). A most remarkable difference to embryonic kidneys existed with regard to the proximal tubules and this could be observed in all studied postnatal kidney stages (and in adult kidney, see below). All segments of the proximal tubules (S1, S2, S3) were equally and intensely stained with PSL (Fig. 4B, E), whereas the S1 and S2 parts of proximal tubules were

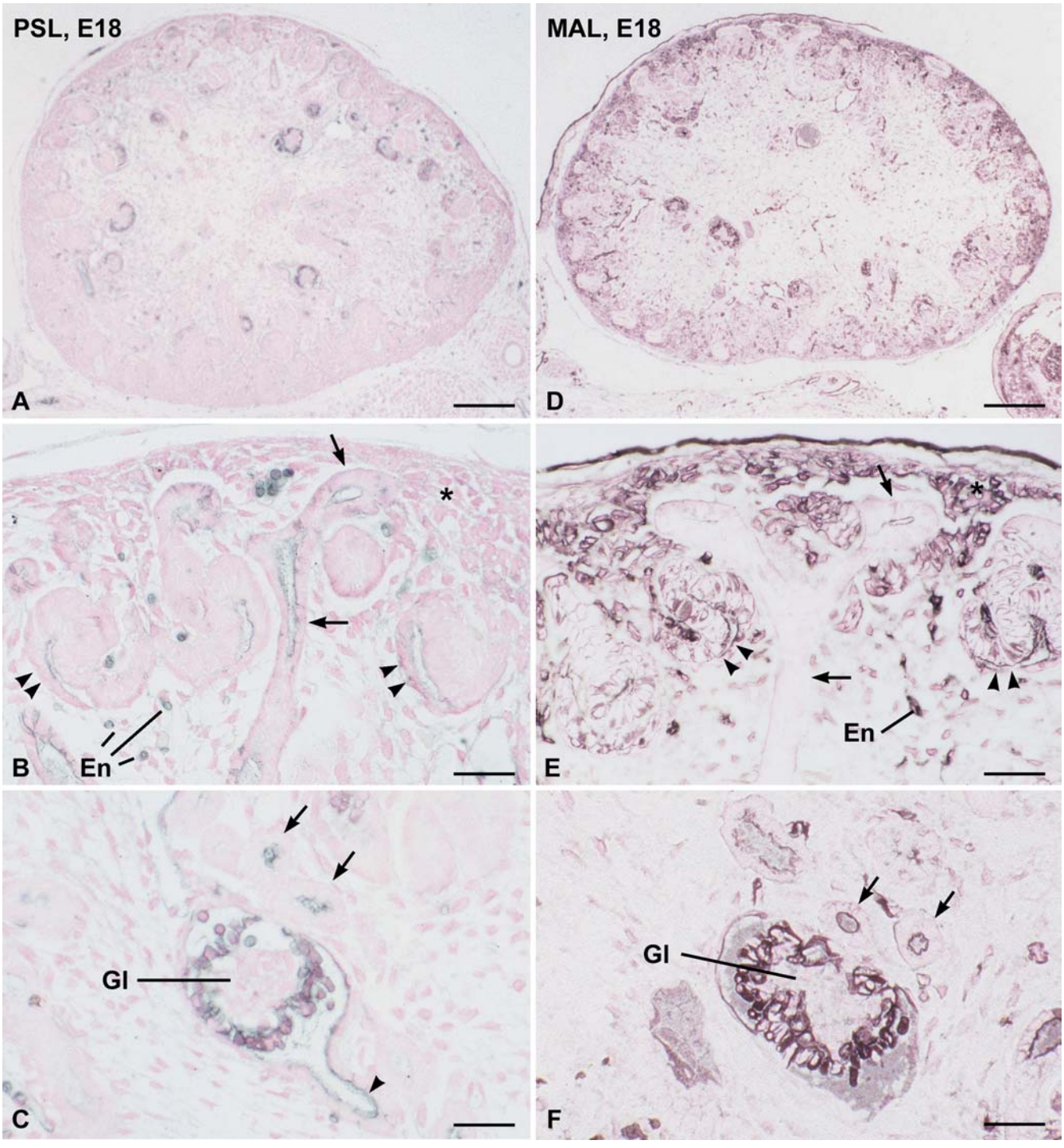

Fig. 2A–F Consecutive sagittal sections of paraffin-embedded rat kidney, embryonic day 18. **A–C** Ureteric bud-derived collecting ducts (*arrows* in **B**), proximal part of S-shaped bodies (*double arrowheads*), immature glomeruli (*Gl*), and immature proximal tubules (*arrowhead* and *arrows* in **C**) are positive for α2,6-linked sialic acid. Condensed metanephrogenic mesenchyme (*asterisk*) and stromal mesenchyme appear unreactive. **D–F** Intense staining for α2,3-linked sialic acid is seen in condensed metanephrogenic mesenchyme (*asterisk*), stromal mesenchyme, entire S-shaped bodies (*double arrowheads* in **E**), immature glomeruli (*Gl*), and immature proximal tubules (*arrows* in **F**). *Arrows* in **E** point to collecting ducts and staining of the terminal ampullae. *En* Positive endothelium. *Bars* 90 μm in **A**, **D**; 25 μm in **B**, **C**, **E**, **F**

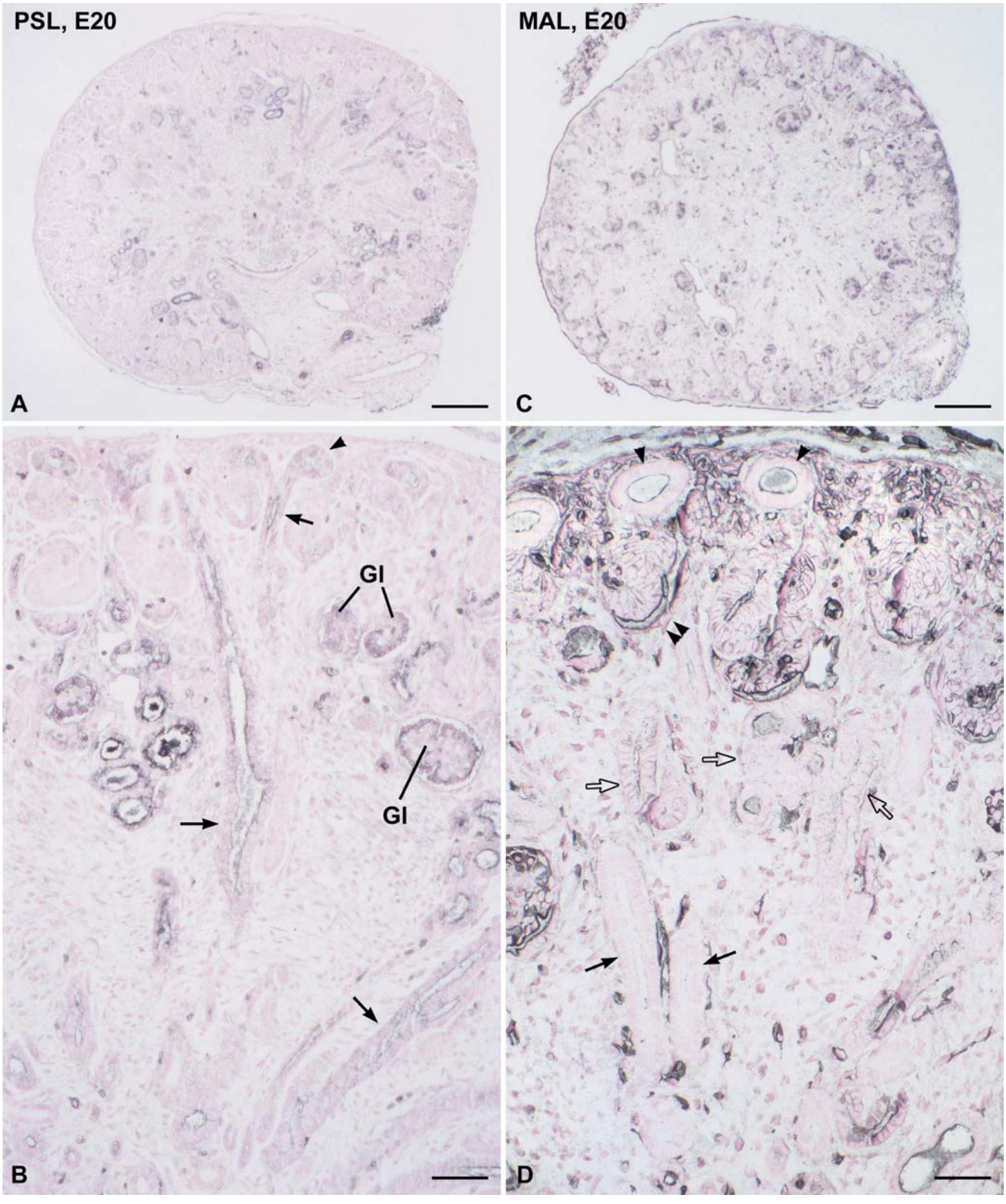

Fig. 3A–D Adjacent sagittal sections of paraffin-embedded rat kidney, embryonic day 20. **A**, **B** Staining pattern for α2,6-linked sialic acid corresponds to that of embryonic day 18. Terminal ampulla (*arrowhead*) of collecting ducts (*arrows*), glomeruli (*Gl*). **C**, **D** Staining pattern for α2,3-linked sialic acid corresponds to that of embryonic day 18. Positive terminal ampulla (*arrowheads*) of unreactive collecting ducts (*arrows*) are seen as well as positive S-shaped bodies (*double arrowheads*), glomeruli, and immature proximal tubules (*open arrows*). *Bars* 90 μm in **A**, **B**; 20 μm in **C**, **D**

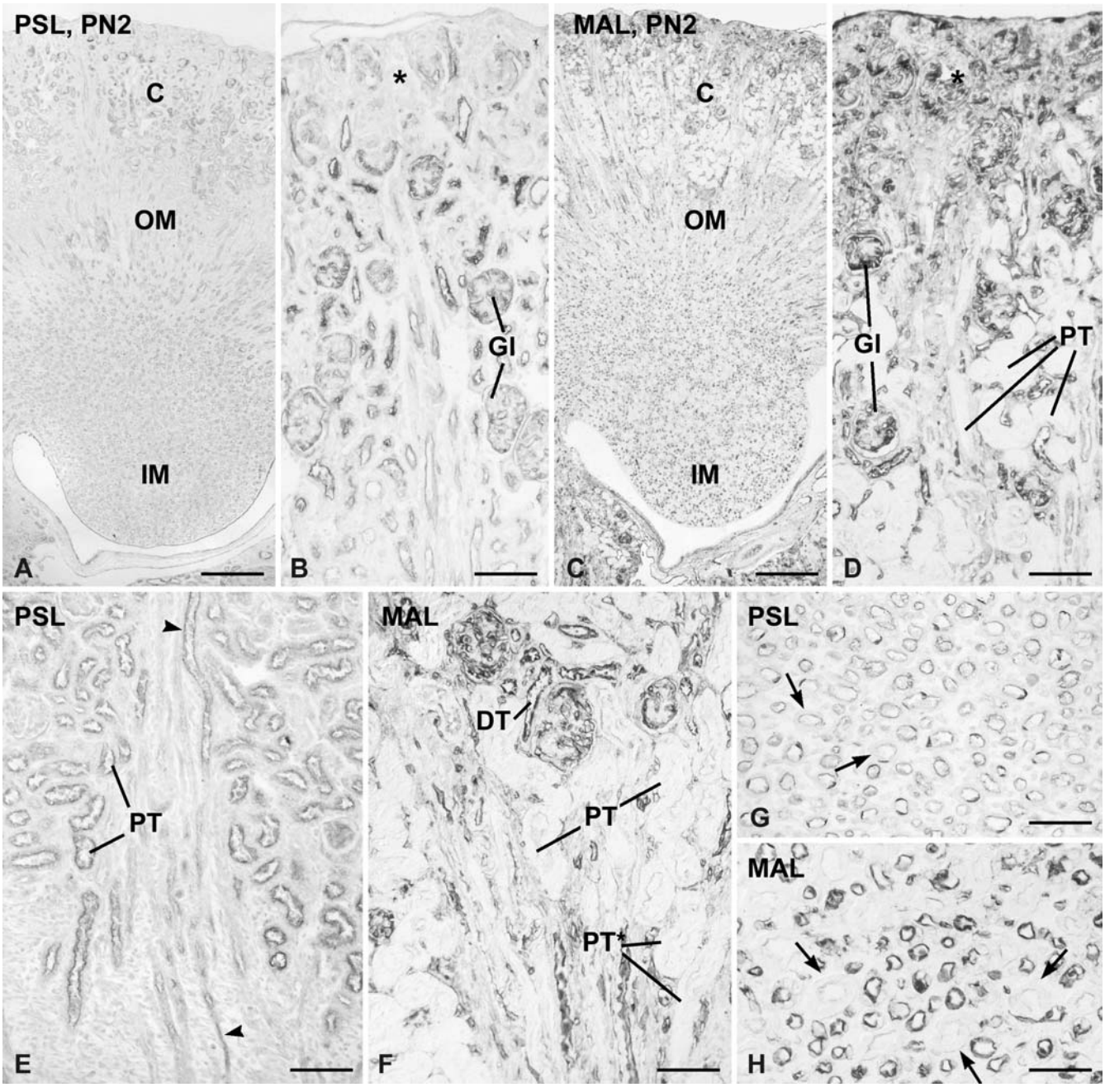

Fig. 4A–H Serial sections of paraffin-embedded rat kidney, postnatal day 2. The general distribution of α2,6-linked sialic acid in cortex (*C*), outer (*OM*), and inner (*IM*) medulla is shown in **A**. **B** is a detail from cortex with nephrogenic zone (*asterisk*). Glomeruli (*Gl*) and proximal tubules are positive. In **C**, the general distribution of α2,3-linked sialic acid in cortex (*C*), outer (*OM*) and inner (*IM*) medulla is shown. **D** represents a detail from cortex with positive nephrogenic zone (*asterisk*) and positive glomeruli (*Gl*); convoluted proximal tubules (*PT*) are unreactive. **E** and **F** show part of cortex with adjacent outer stripe of outer medulla. Although convoluted (*PT* in **E**) and straight (*arrowheads* in **E**) proximal tubules are positive for α2,6-linked sialic acid; reactivity for α2,3-linked sialic acid is undetectable in convoluted proximal tubules (*PT* in **F**) and only faint staining is detectable in straight proximal tubules (*PT**). *DT* Positive distal tubule. **G**, **H** Details of inner medulla showing that all structures are reactive for α2,6-linked sialic acid (**G**) and α2,3-linked sialic acid (**H**) although the staining for the former is weak. *Arrows* in **G** and **H** point to positive large collecting ducts. *Bars* 280 μm in **A**, **C**; 60 μm in **B**, **D**, **G**, **H**; 45 μm in **E**, **F**

unreactive with MAL (*PT* in Fig. 4D). Only S3 of proximal tubules were faintly MAL positive (*PT** in Fig. 4F). This differential PSL and MAL staining of proximal tubules is illustrated for postnatal day 7 in Fig. 5 and postnatal day 21 in Fig. 6. Thin loops of Henlé and distal tubules as well as intertubular capillaries of the examined postnatal stages were positive with both PSL and MAL (Figs. 4, 5, 6). The stromal cells were largely

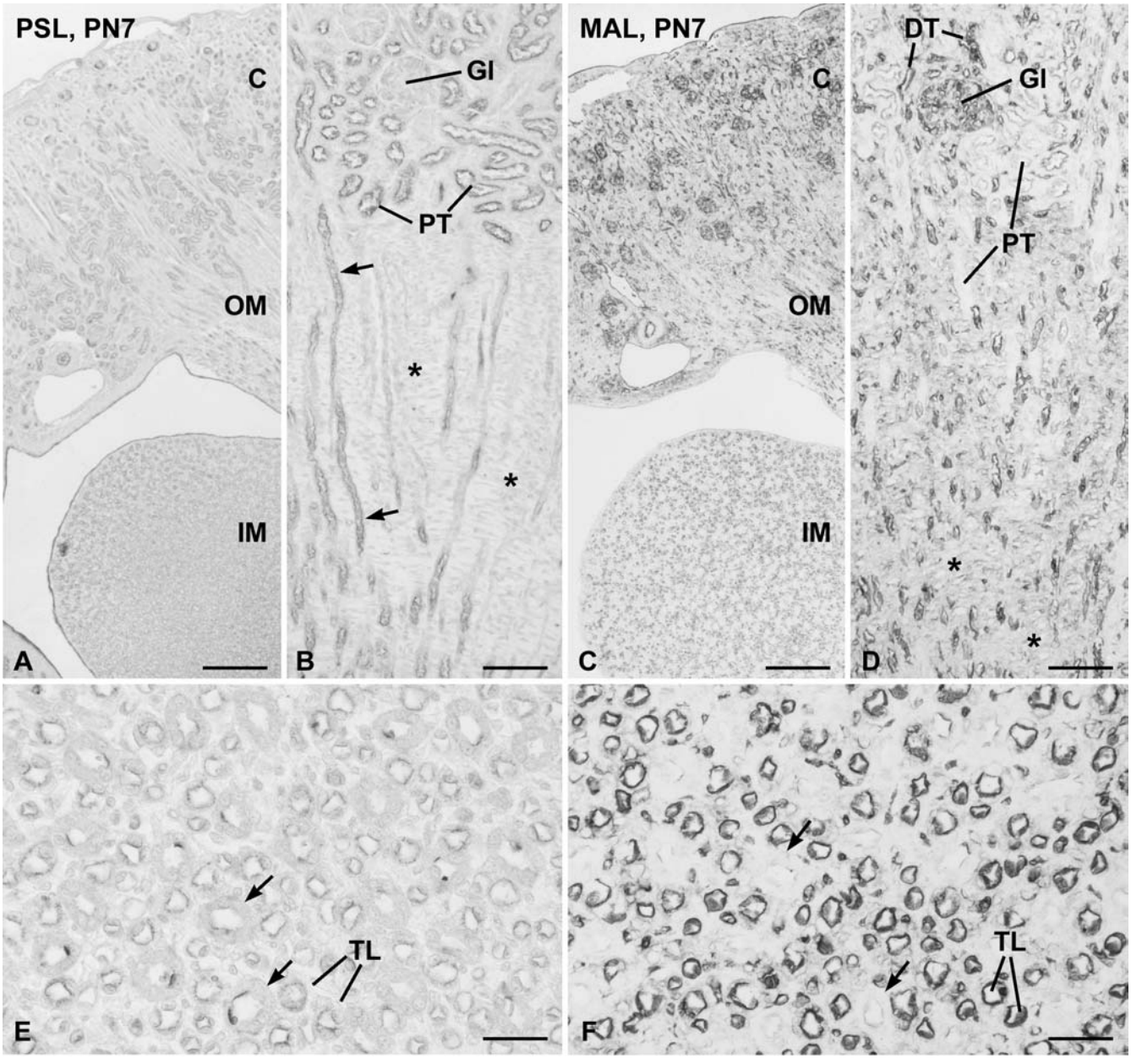

Fig. 5A–F Serial sections of paraffin-embedded rat kidney, postnatal day 7. At low magnification, the distribution of α2,6-linked sialic acid (**A**) and of α2,3-linked sialic acid (**C**) in cortex (*C*), outer (*OM*) and inner (*IM*) medulla is seen. In the cortex, staining for α2,6-linked sialic acid (**B**) is present in glomeruli (*Gl*) and convoluted (*PT*) as well as straight (*arrows*) proximal tubules. Stromal mesenchyme (*asterisks*) appears unreactive. Although glomeruli (*Gl*), distal tubules (*DT*), and stromal mesenchyme (*asterisks*) are positive for α2,3-linked sialic acid (**D**), proximal tubules (*PT*) are unreactive. In inner medulla, all structures are weakly positive for α2,6-linked sialic acid (**E**) whereas all elements with the exception of large collecting ducts (*arrows*) were strongly positive for α2,3-linked sialic acid (**F**). *TL* Thin loops. *Bars* 200 μm in **A**, **C**; 45 μm in **B**, **D**; 30 μm in **E**, **F**

unreactive with PSL (Figs. 4E, 5B) but stained by MAL (Figs. 4F, 5D). Likewise, the collecting ducts of cortex and outer as well as inner medulla were reactive for both PSL and MAL (Figs. 4, 5, 6).

The de-*O*-acetylation of sialic acids by saponification of tissue sections had no influence on intensity and pattern of lectin staining (data not shown).

Distribution pattern of α2,6- and α2,3-linked sialic acid in adult kidneys

To achieve the highest spatial resolution and morphological comparability, consecutive serial semithin sections of Lowicryl K4 M-embedded kidney were investigated. Although the staining pattern of proximal tubules for PSL and MAL in adult kidney corresponded to that observed

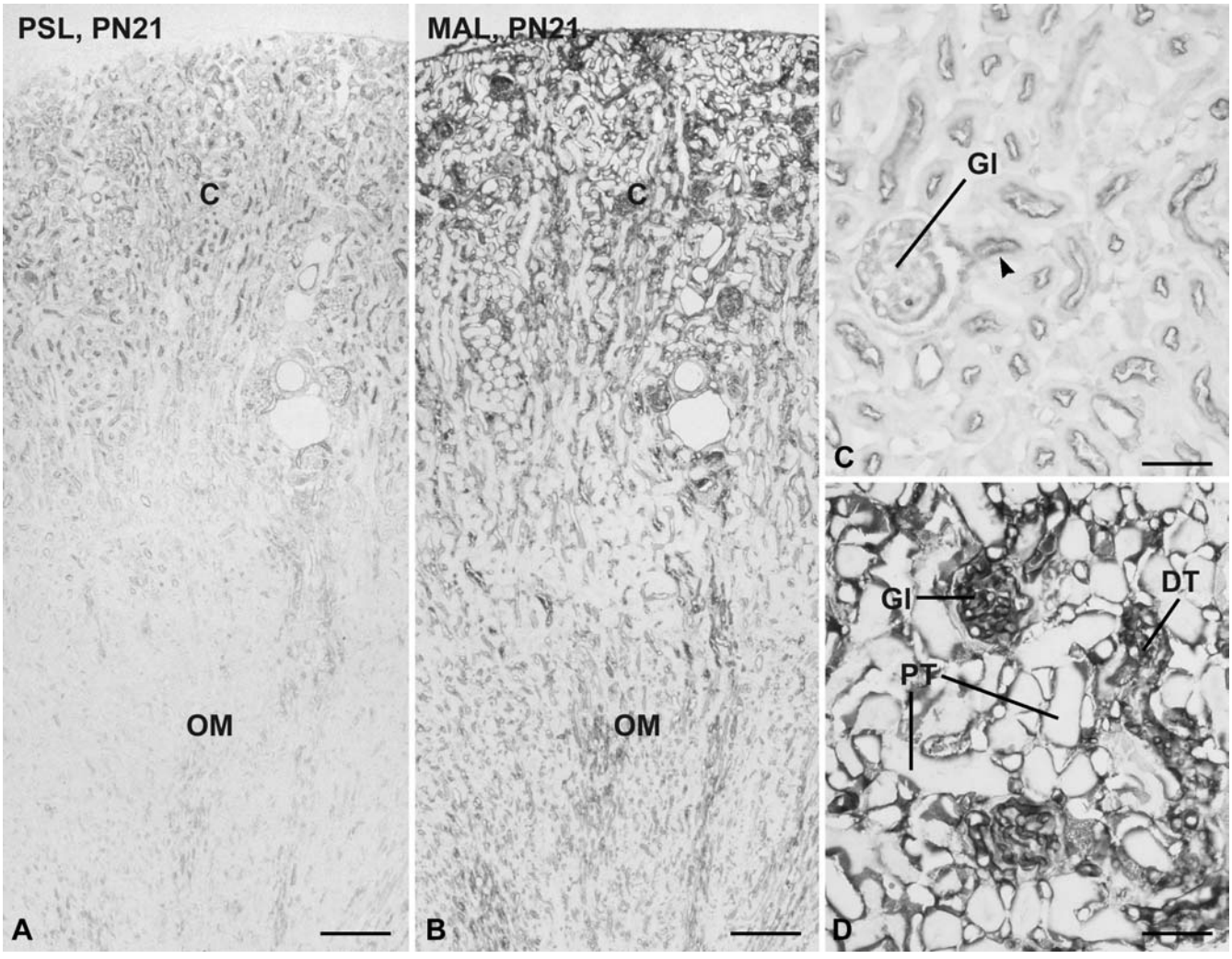

Fig. 6A–D Serial sections of paraffin-embedded rat kidney postnatal day 21. Low magnification showing staining for α2,6-linked sialic acid (**A**) and α2,3-linked sialic acid (**B**) in cortex (*C*) and adjacent outer medulla (*OM*). Details from cortex with glomeruli (*Gl*) and proximal tubules (*arrowhead* points to the origin of proximal tubule) positive for α2,6-linked sialic acid (**C**). Although glomeruli (*Gl*) and distal tubules (*DT*) are positive for α2,3-linked sialic acid (**D**), proximal tubules (*PT*) in cortex are unreactive. *Bars* 120 μm in **A**, **B**; 40 μm in **C**, **D**

from postnatal day 2 onward, subtle changes in the collecting ducts were noted.

In the cortex, the glomeruli, parietal Bowman's capsule, proximal and distal tubules with the loops of Henlé in between and including the macula densa, cortical collecting ducts, and intertubular capillaries as well as small arteries and veins were positive with PSL (Fig. 7A–C). Proximal tubules stained stronger with PSL than distal tubules and cortical collecting ducts (Fig. 7B). Glomeruli were also positive for MAL but the staining was confined to the endothelia with the podocytes and mesangial cells being unreactive (compare Fig. 7F and C). As already observed in postnatal kidneys, the S1 and S2 segments of proximal tubules were unreactive with MAL (compare Fig. 7E, F and B, C). In contrast, the S3 of proximal tubules was weakly MAL positive (compare Fig. 8E and B). Thin loops were reactive with both lectins (Figs. 8, 10). Distal tubules and collecting ducts in cortex and outer medulla as well as capillaries and small arteries and veins were stained with MAL (Fig. 7E, F). Although the epithelia lining the collecting ducts in cortex and outer as well as inner medulla were reactive with PSL (Fig. 8B, C), a mosaic of MAL-positive and MAL-negative epithelia in cortical and outer medulla collecting ducts was clearly visible (Figs. 8E, F, 9A–C). By electron microscopy, the intercalated cells were identified as the MAL-positive cells (Fig. 9D). In Fig. 10, a detail of the inner medulla is presented. The large collecting duct principal cells were unreactive with MAL, whereas epithelia of thin loops and capillary endothelia were labeled.

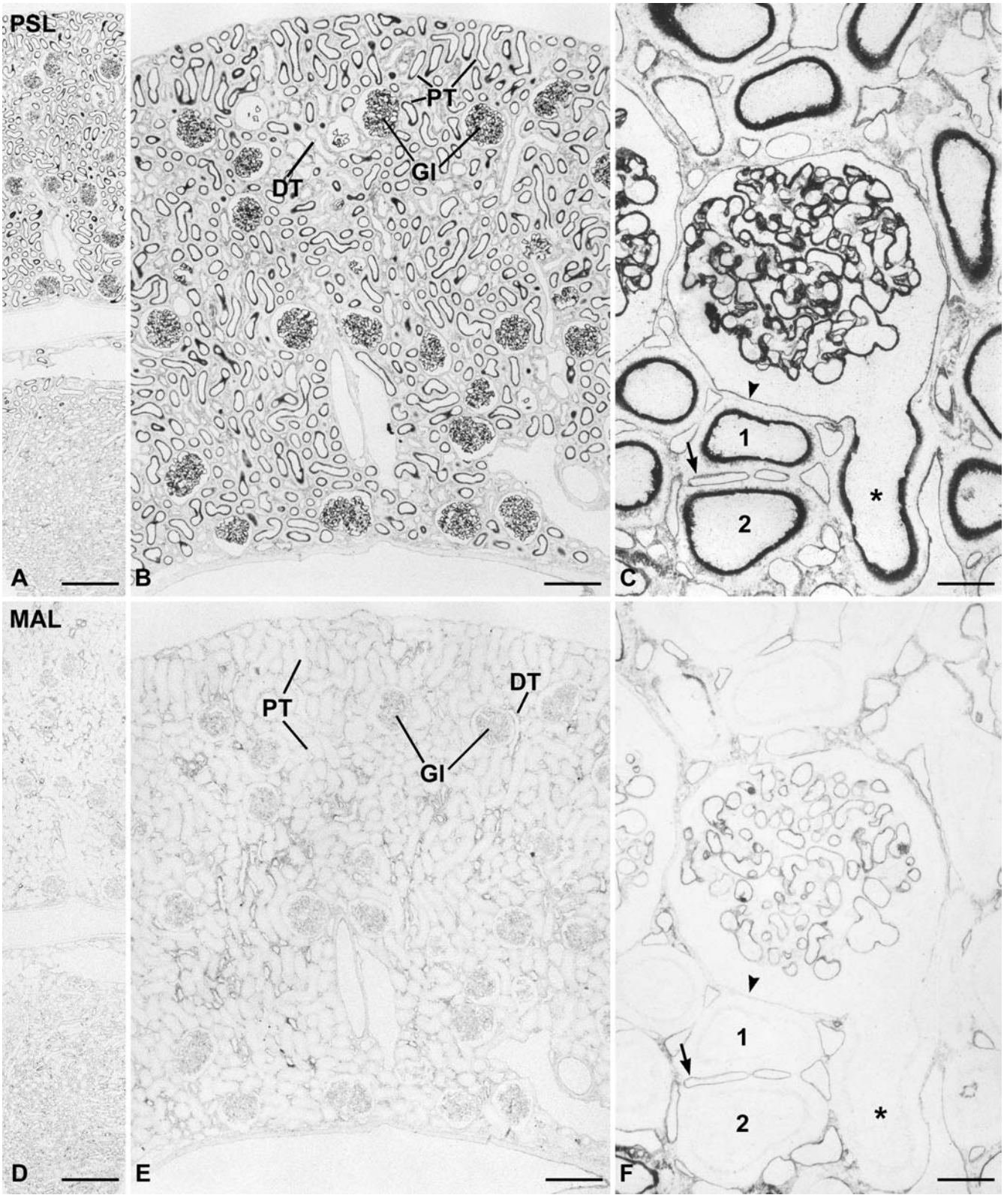

Fig. 7A–F Consecutive serial semithin sections from Lowicryl K4 M-embedded adult rat kidney. General staining pattern for α2,6-linked sialic acid (**A**) and of α2,3-linked sialic acid (**D**) in cortex and adjacent outer medulla. Glomeruli (*Gl*) as well as proximal (*PT*) and distal tubules are intensely stained for α2,6-linked sialic acid (**B**) whereas staining for α2,3-linked sialic acid (**E**) in glomeruli (*Gl*) and distal tubules (*DT*) is weak and absent in proximal tubules (*PT*). High power magnification reveals that podocytes, endothelia, and mesangial cells of glomeruli are positive for α2,6-linked sialic acid (**C**) whereas only the endothelia of glomeruli are positive for α2,3-linked sialic acid (**F**). The origin of the proximal tubule at the urinary pole (*asterisk* in **C** and **F**) and cross-sectioned profiles of the same segment S1 of proximal tubules (*1*, *2* in **C** and **F**) are reactive for α2,6-linked sialic acid (**C**) and not for α2,3-linked sialic acid (**F**). *Arrowhead* Parietal Bowman's capsule, *arrow* cross-sectioned intertubular capillaries. *Bars* 50 μm in **A**, **D**; 20 μm in **B**, **E**; 5 μm in **C**, **F**

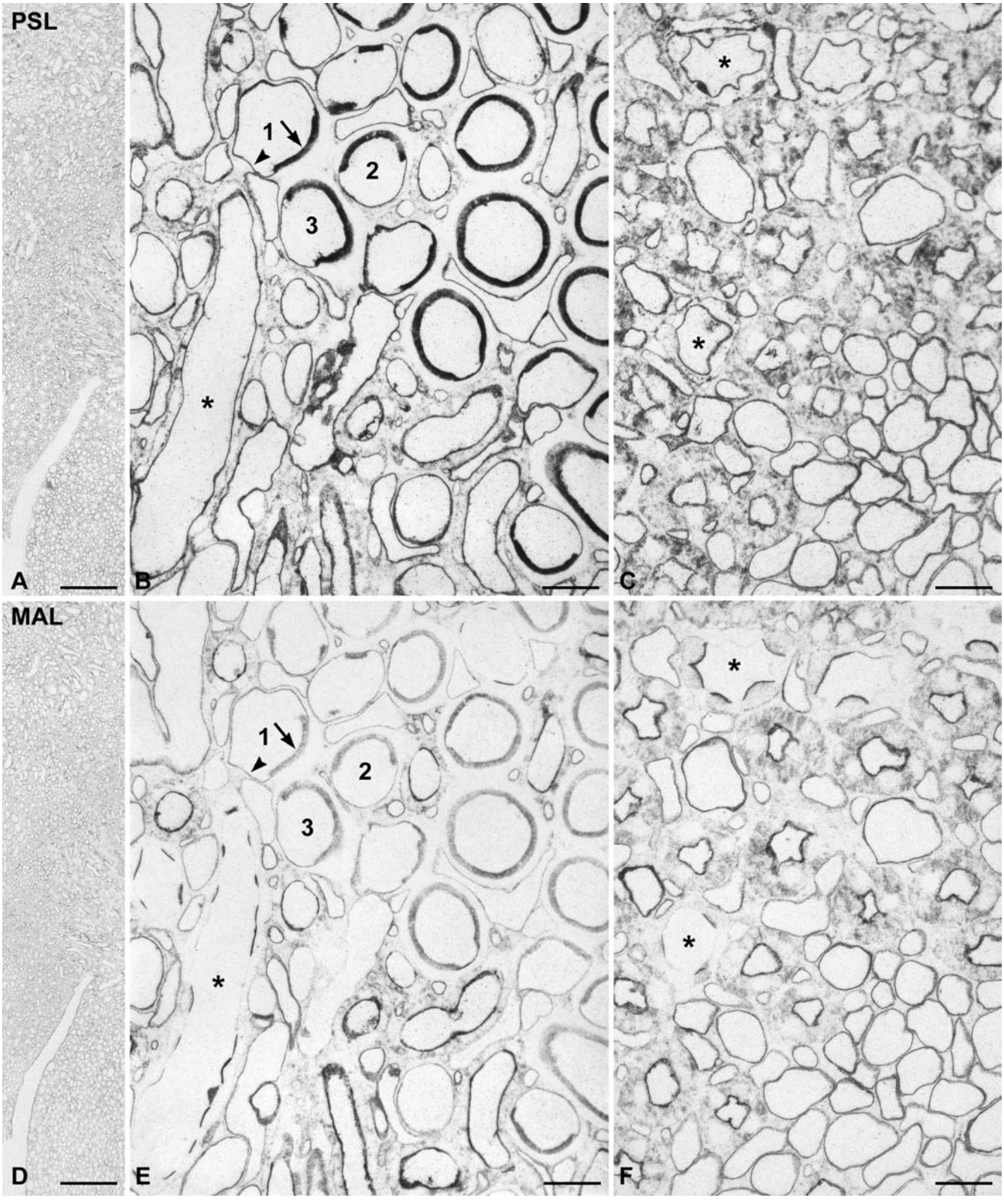

Fig. 8A–F Consecutive serial semithin sections from Lowicryl K4 M-embedded adult rat kidney. General staining pattern for α2,6-linked sialic acid (**A**) and of α2,3-linked sialic acid (**D**) in parts of outer and inner medulla. **B**, **E** Cross-sectioned profiles of the same tubules (*1–3* in **B** and **E**) showing transition of S3 segment of proximal tubule (*arrow* in **B** and **E**) in descending thin loop (*arrowhead* in **B** and **E**) are positive for both α2,6-linked sialic acid (**B**) and α2,3-linked sialic acid (**E**). All epithelia of collecting ducts are positive for α2,6-linked sialic acid (*asterisk* in **B** and **C**) whereas the same collecting ducts exhibit a mosaic of cells positive and negative for α2,3-linked sialic acid (*asterisk* in **E** and **F**). Loops of Henlé and capillaries are positive for both α2,6- and α2,3-linked sialic acid (**C** and **F**). *Bars* 50 μm in **A**, **D**; 5 μm in **B**, **C**, **E**, **F**

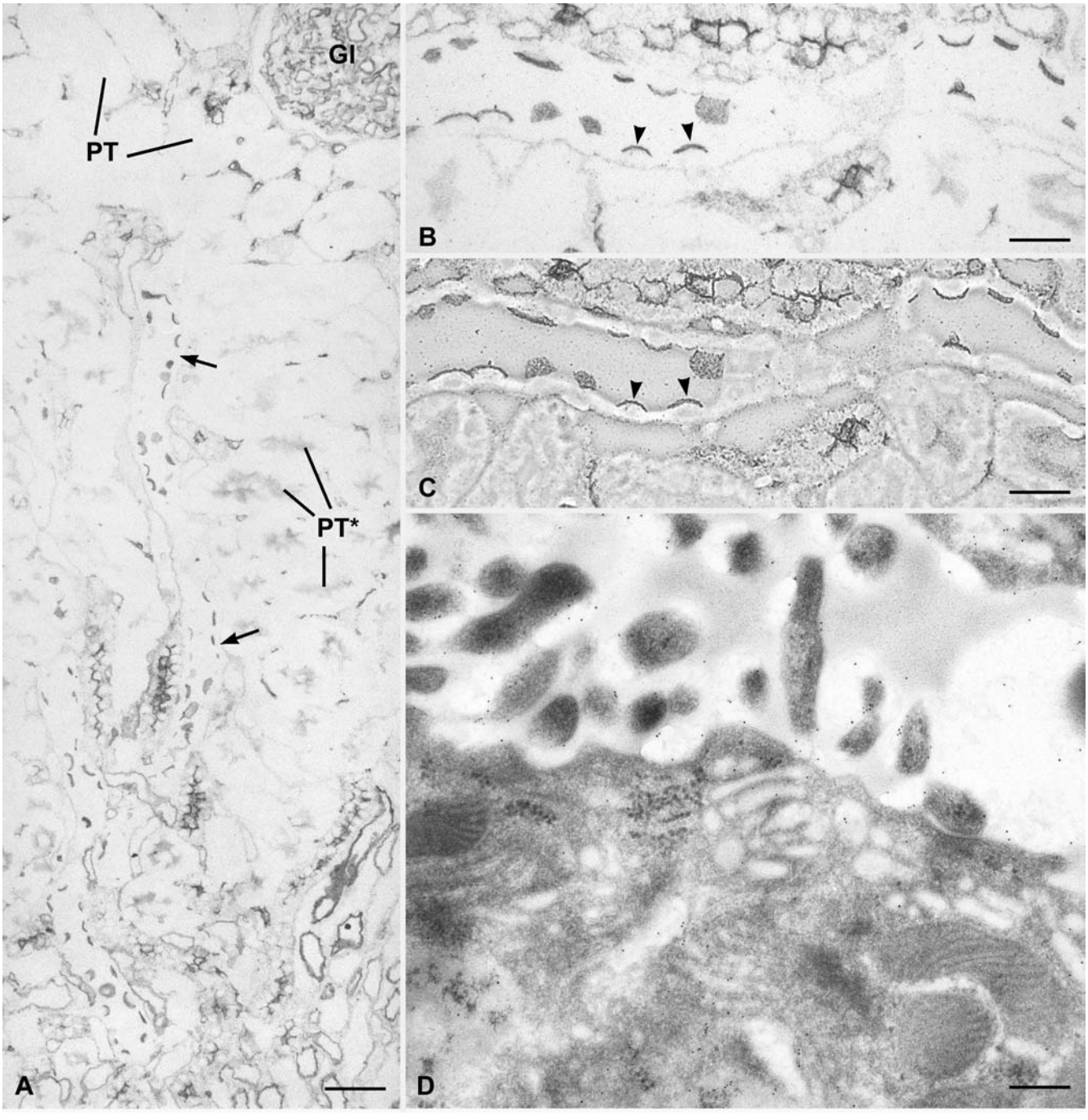

Fig. 9A–D Adult rat kidney, Lowicryl K4 M embedding, detection of α2,3-linked sialic acid. Detail from cortex and outer medulla with glomerulus (*Gl*) and unreactive S1 and S2 proximal tubules (*PT*) as well as weakly stained S3 proximal tubules (*PT**). Collecting ducts (*arrows* in **A**) with a mosaic of positive (*arrowheads* in **B** and **C**) and negative cells are seen at higher magnification in **B** and **C**. The positive cells were identified as intercalated cells by electron microscopy and MAL–gold labeling (**D**). *Bars* 15 μm in **A**; 10 μm in **B**, **C**; 0.25 μm in **D**

Sialyltransferase activities in embryonic, postnatal, and adult kidney

A more than threefold difference in specific activity between β-galactoside α2,6 sialyltransferase (ST6Gal-I) and β-galactoside α2,3 sialyltransferase (ST3Gal-III) was measured in aliquots of pooled homogenates from embryonic day 20 kidneys (Fig. 11). Although activity levels of both sialyltransferases decreased postnatally, the one for β-galactoside α2,6 sialyltransferase was always higher and decreased steadily, whereas the activity levels for β-galactoside α2,3 sialyltransferase remained steady from postnatal day 5 onward. As compared to embryonic and postnatal kidneys, activity levels for both sialyltrans-

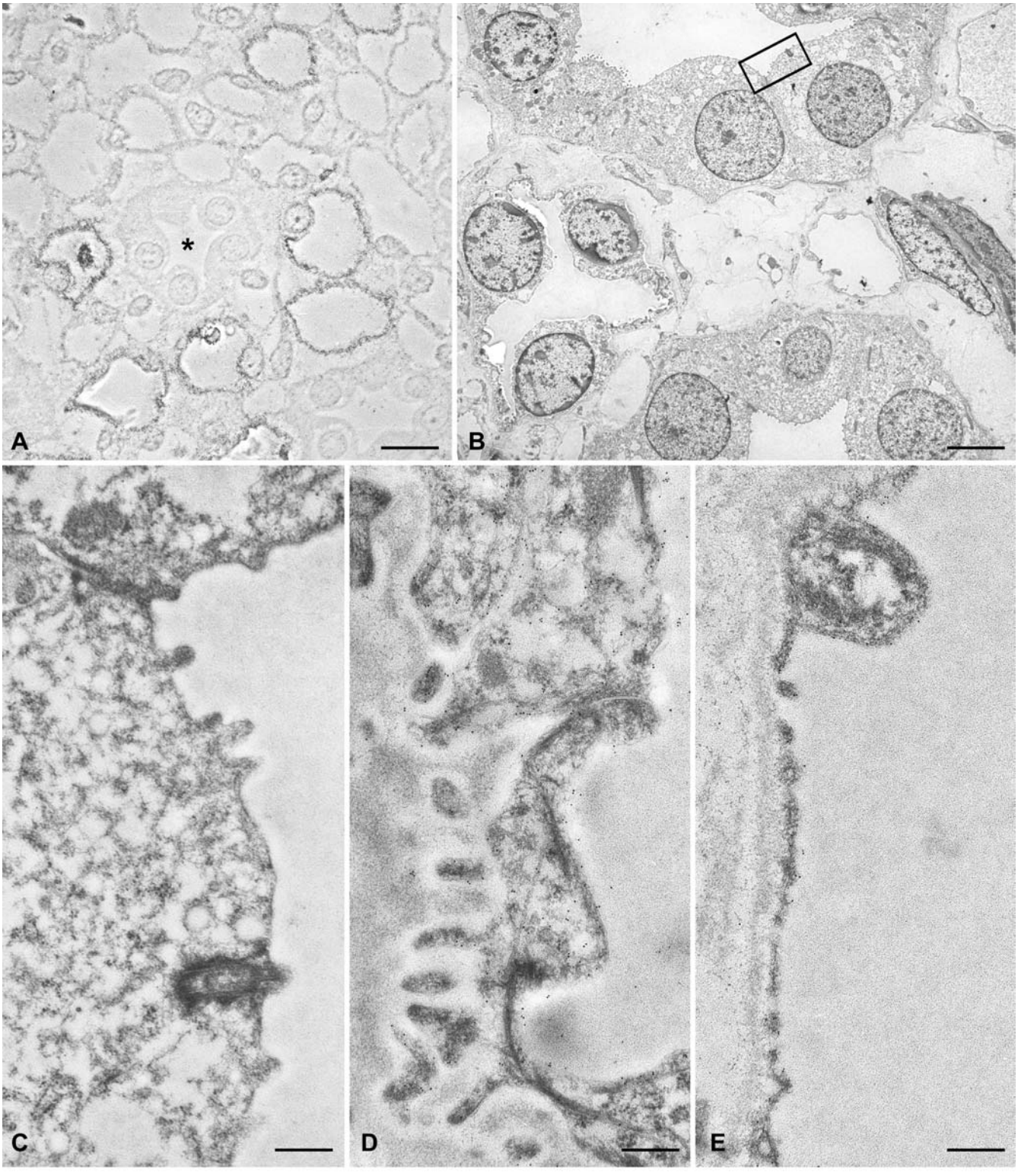

Fig. 10A–E Details from inner medulla of adult rat, Lowicryl K4 M embedding, detection of α2,3-linked sialic acid. Principal cells of collecting ducts (*asterisk* in **A**) are unreactive and this was confirmed by electron microscopic MAL–gold labeling (**B**, **C**), whereas gold particle labeling was detectable in thin loops (**D**) and endothelia of capillary (**E**). *Bars* 8 μm in **A**; 2 μm in **B**; 0.25 μm in **C**; 0.3 μm in **D**, **E**

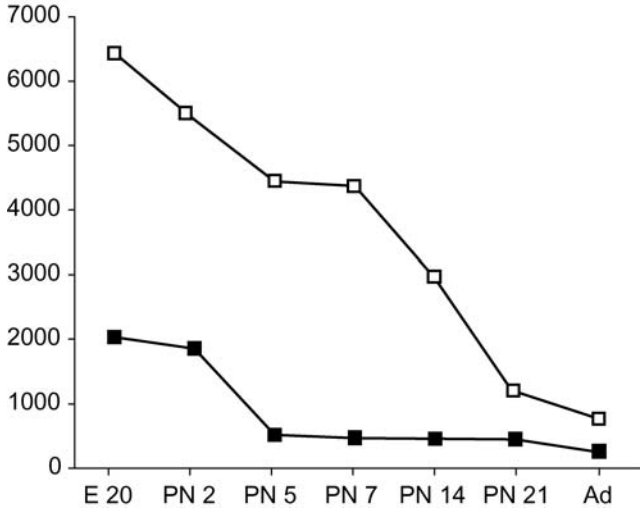

Fig. 11 Enzyme activity levels for β-galactoside α2,6 sialyltransferase (*open squares*) and β-galactoside α2,3 sialyltransferase (*filled squares*) in embryonic (*E*), postnatal (*PN*), and adult (*Ad*) kidneys. Enzyme activity levels are expressed as picomoles of [^{14}C] NeuAc transferred per milligram of acceptor substrate per hour

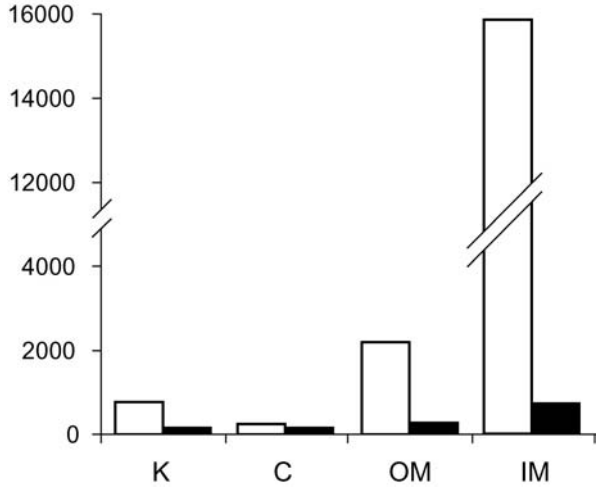

Fig. 12 Enzyme activity levels for β-galactoside α2,6 sialyltransferase (*open columns*) and β-galactoside α2,3 sialyltransferase (*filled columns*) in whole adult kidney (*K*), dissected cortex (*C*), outer medulla (*OM*), and inner medulla (*IM*). Enzyme activity levels are expressed as picomoles of [^{14}C] NeuAc transferred per milligram of acceptor substrate per hour

ferases were lowest in adult kidney. The activity for β-galactoside α2,6 sialyltransferase as compared to that of β-galactoside α2,3 sialyltransferase was almost fourfold higher in homogenates prepared from whole kidneys (Fig. 11). When microscopically dissected cortex, outer medulla, and inner medulla were assayed separately, activity for both sialyltransferases was lowest in cortex and highest in inner medulla (Fig. 12). Although activity for β-galactoside α2,6 sialyltransferase as compared to β-galactoside α2,3 sialyltransferase was higher in all three regions, this difference was most striking in inner medulla.

Lectin blot analysis of embryonic, postnatal, and adult kidney

The aim of this analysis was to establish solely the pattern of PSL- and MAL-reactive glycoproteins and not to identify specific glycoproteins.

Although different from each other, the pattern of reactive bands for PSL and MAL was remarkably steady when homogenates of whole kidneys from embryonic day 20, postnatal days 2–21, and adult kidney were investigated (Fig. 13). Interestingly, only few major reactive bands were detected in the 3–15% gradient gels. A band with an approximate molecular mass of 200 kDa was reactive with both PSL and MAL. Although its reactivity with MAL was observed in embryonic day 20 and all postnatal stages studied as well as in adult kidney,

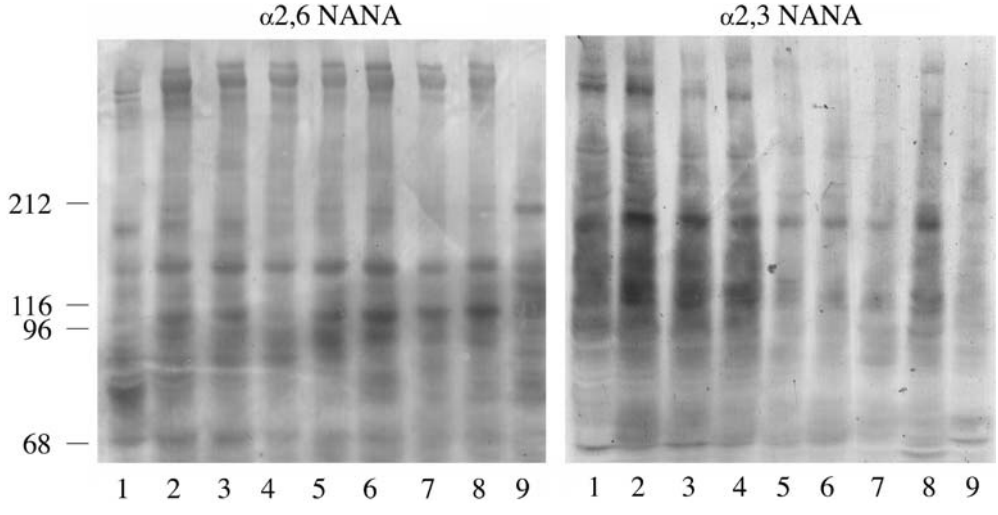

Fig. 13 Lectin blot analysis of glycoproteins bearing α2,6-linked sialic acid (*α2,6 NANA*) and α2,3-linked sialic acid (*α2,3 NANA*), kidney homogenates resolved in 3–15% SDS-polyacrylamide gels. *Lanes 1* Embryonic day 20, *lanes 2* postnatal day 2, *lanes 3* postnatal day 5, *lanes 4* postnatal day 7, *lanes 5* postnatal day 14, *lanes 6* postnatal day 21, *lanes 7* whole adult kidney, *lanes 8* adult kidney cortex, *lanes 9* adult kidney inner medulla

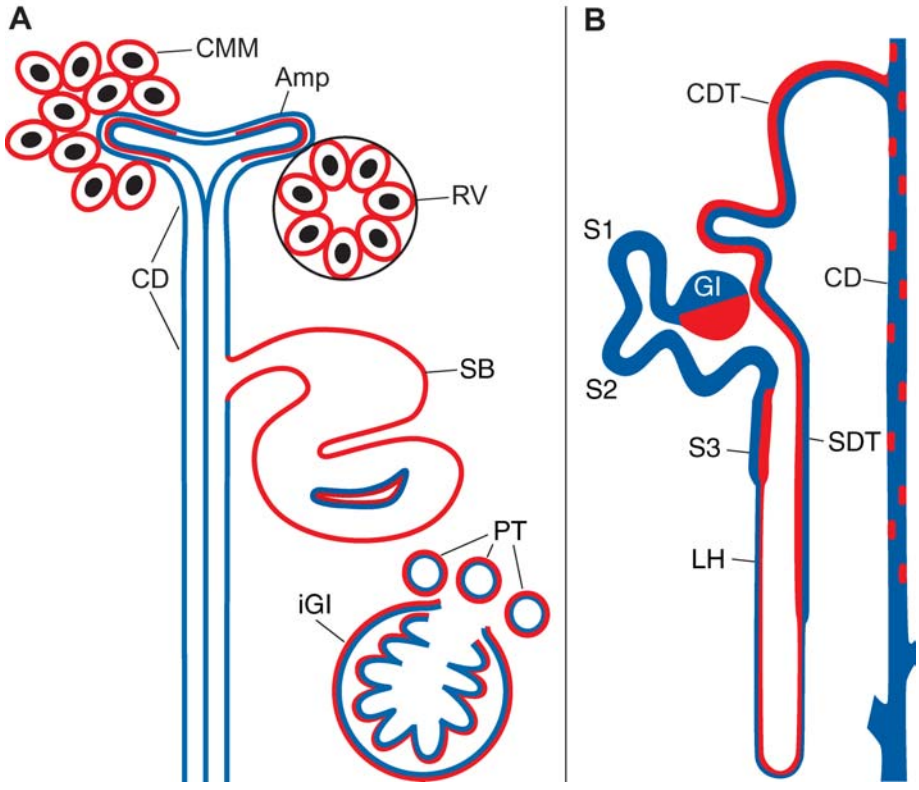

Fig. 14A, B Schematic presentation of the distribution of α2,6- and α2,3-linked sialic acids in embryonic and adult rat kidney. **A** Embryonic kidney with condensed metanephrogenic mesenchyme (*CMM*), renal vesicle (*RV*), S-shaped body (*SB*), immature glomerulus (*iGl*), immature proximal tubule (*PT*), collecting duct (*CD*), and ampulla of collecting duct (*Amp*). **B** Adult kidney with glomerulus (*Gl*), S1–S3 segment of proximal tubule (*S1*, *S2*, *S3*), loop of Henlé (*LH*), straight distal tubule (*SDT*), convoluted distal tubule (*CDT*), and collecting duct (*CD*). *Blue coloration* in **A** and **B** indicates presence of α2,6-linked sialic acid as detected with PSL and SNL, whereas *red* represents α2,3-linked sialic acid as detected with MAL

it became undetectable with PSL from postnatal day 7 onward. One of the high molecular mass bands seen in all samples (except for medulla) apparently represents megalin in cortex (Christensen et al. 1995; Farquhar et al. 1995; Kerjaschki and Farquhar 1982), which has previously been shown to carry both α2,6- and α2,3-linked sialic acids (Morelle et al. 2000; Ziak et al. 1999). When microscopically dissected cortex and inner medulla of adult kidney were probed with PSL and MAL, remarkable differences were observed between the lectins and the kidney regions investigated (Fig. 13 *lanes 8, 9*).

Discussion

In the present study, we showed that: (a) *N*-glycans terminated in α2,6- and α2,3-linked sialic acid as well as activity for the respective sialyltransferases are detectable in embryonic, postnatal, and adult kidney, (b) that α2,6- and α2,3-linked sialic acids are differently expressed in the two embryonic anlagen and in the mesenchyme-derived early stages of nephron morphogenesis (Fig. 14A), and (c) that regional and cell type-specific differences exist in adult kidney (Fig. 14B). Lectin blot analysis revealed steady patterns of bands reactive for α2,6- and α2,3-linked sialic acids from embryonic to postnatal and adult kidneys. The activity of both the β-galactoside α2,6 sialyltransferase and β-galactoside α2,3 sialyltransferase declined from embryonic over postnatal to adult kidney. The activity for β-galactoside α2,6 sialyltransferase was always three to fourfold higher than β-galactoside α2,3 sialyltransferase.

The present lectin histochemical results indicate that distinct patterns of expression of α2,6- and α2,3-linked sialic acids exist during embryonic metanephron formation and postnatal kidney differentiation. One concerns the metanephrogenic mesenchyme which was reactive with MAL, but not with PSL and SNL, from embryonic day 16 until about postnatal day 5 after which nephrogenesis in rat kidney ceases. This indicates that the condensed metanephrogenic mesenchyme is rich in *N*-glycans bearing α2,3-linked sialic acids. This was also observed for the loose mesenchyme in embryonic, postnatal, and adult kidney. In contrast, α2,6-linked sialic acids were absent from this embryonic anlage or existed in amounts too low to be detectable with PSL and SNL. Likewise, the loose mesenchyme was unreactive with PSL and SNL in embryonic, postnatal, and adult kidney. In this regard, the only other studied sialoglycoconjugates were the polyα2,8-neuraminic acid on NCAM (Lackie et al. 1990; Roth et al. 1987) and the oligo/poly α2,8-KDN of megalin (Ziak and Roth 1999) which exhibited a mutually exclusive distribution with the polyα2,8-neuraminic acid being detectable in the metanephrogenic mesenchyme. A local mediator of signaling events during metanephrogenic mesenchyme induction is *WT1* and together with *Wnt-4* is representative of the very few genes expressed in the mesenchyme but not in the ureteric bud (Armstrong et al. 1993; Bard et al. 1994; Kispert et al. 1998; Kreidberg et al. 1993; Stark et al. 1994).

Another difference in expression of α2,6- and α2,3-linked sialic acids concerns the mesenchyme–epithelium transition and glomerulus morphogenesis. All stages of nephron formation were reactive with MAL, as shown previously with the sialic acid specific *Limax flavus* lectin (Wagner and Roth 1988) and for polyα2,8-neuraminic acid on NCAM (Lackie et al. 1990; Roth et al. 1987). In contrast, the renal vesicle, which represents the first epithelial differentiation, was unreactive with PSL and SNA. The S-shaped body which consists of a proximal and a distal portion gives raise to the glomerulus and tubular part of the nephron, respectively, exhibited PSL and SNL staining only in the presumptive visceral (podocytes) and parietal Bowman's epithelium which coincides with transient labeling by GalNAc-reactive lectins (Laitinen et al. 1987) and the expression of WT-1 (Horster et al. 1999). However, immature proximal tubules occurring with the capillary loop stage were then reactive with both PSL and SNL. This indicates that α2,6-linked sialic acids occur rather late in early nephrogenesis and initially are cell type restricted. They are, however, maintained during maturation of the tubule epithelium and persist in adult kidney. This contrasts with the MAL reactivity in proximal tubules which is transient during embryonic development and no longer observed in S1 and S2 segments of mature proximal tubules from postnatal day 2 kidneys onward. A similar transient expression of polyα2,8-neuraminic acid on NCAM was observed in chicken and rat kidney (Lackie et al. 1990; Thiery et al. 1982). With regard to the mechanism of remodeling of the S-shaped body which results in the formation of a double slit, changes in cell–cell contact and adhesiveness have been postulated to be involved (Hilfer and Hilfer 1983; Kiremidjian and Kopac 1972). One might speculate that negatively charged sialic acids are involved in this process (Lackie et al. 1990; Roth et al. 1987; Ziak and Roth 1999; present study).

The ureteric bud and its ramification give rise to the collecting duct system. Both, PSL and SNL staining indicative of the presence of α2,6-linked sialic acids were detectable in the entire collecting duct system of embryonic kidneys in contrast to the metanephrogenic mesenchyme. Staining persisted in postnatal kidneys and was observed in collecting ducts of adult kidneys as well. However, MAL staining indicative of α2,3-linked sialic acids was detectable only in the terminal ampullae (tips) of the collecting ducts during embryonic days 16, 18, and 20. This resembled the reported restricted expression of polyα2,8-neuraminic acid on NCAM (Lackie et al. 1990) and coincides with the expression of *Wnt-11* (Horster et al. 1999).

The observed changing pattern of α2,6- and α2,3-linked sialic acids as detected by lectin histochemistry during induction, nephrogenesis, and differentiation in embryonic and postnatal rat kidneys revealed a high degree of cell type-specific expression during these processes. Their functional importance remains to be investigated. Due to the terminal position of sialic acids in glycans at the cell surface, it has been suggested that they are involved in cell–cell interactions during embryonic differentiation and functional maturation in adult organs. The regulated expression of a Gal β1,3 GalNAc α2,3 sialyltransferase in developing thymocytes and during T lymphocyte activation (Gillespie et al. 1993; Priatel et al. 2000) and the control of lymphocyte activation by the Gal β1,4 GlcNAc α2,6 sialyltransferase provide appropriate examples (Hennet et al. 1998). However, in Gal β1,4 GlcNAc α2,6 sialyltransferase knockout mice, biological defects in addition to those of B and T lymphocytes are unknown at present (Martin et al. 2002).

In adult kidney, all cells of the nephron and the collecting duct system expressed α2,6-linked sialic acids and this correlates well with previously published data of Gal β1,4 GlcNAc α2,6 sialyltransferase immunohistochemistry (Burger et al. 1998; Kaneko et al. 1995) and SNL staining (Kaneko et al. 1995). In contrast, expression of α2,3-linked sialic acid of *N*-glycans in kidney cortex was much more limited. We previously reported an even more restricted expression of α2,3-linked sialic acid of *O*-glycans in cortex and parts of medulla (Toma et al. 1999). Based on the intensity of staining and abundance of positive structures, kidney cortex contains α2,6-linked sialic acid of *N*-glycans in higher amounts than α2,3-linked sialic acid which is in contrast to most other organs. Based on the same histochemical criteria, the kidney medulla appears to contain similar amounts of α2,6- and α2,3-linked sialic acids of *N*-glycans. At the cellular level, other remarkable differences existed. Proximal tubular epithelia in S1 and S2 segments were unreactive with MAL, whereas those in S3 segment were positive for α2,3-linked sialic acid. To our knowledge, the only other example of such a drastic difference in glycocalyx composition in a single cell type depending on its position in the nephron are the intercalated cells of collecting ducts with regard to reactivity toward the *Helix pomatia* lectin (Brown et al. 1985). Although the principal and intercalated cells of collecting ducts were positive with PSL, SNL, and MAL in all studied embryonic and postnatal stages, in adult kidney, principal cells were reactive with PSL and SNL but not with MAL. Thus, our study revealed that regional and cell type-related expression patterns for α2,6- and α2,3-linked sialic acids of *N*-glycans are characteristic features of rat kidney.

By immunocytochemistry, Gal β1,4 GlcNAc α2,3 sialyltransferase immunoreactivity was detected in S1 and S2 segments of proximal tubules and in principal cells of collecting ducts (Burger et al. 1998). We were unable to detect the product of this sialyltransferase in these regions. The most plausible explanation could be that this is the result of competition between the β-galactoside α2,6 sialyltransferase and β-galactoside α2,3 sialyltransferase for the common donor substrate. In this regard, we found higher activity levels for Gal β1,4 GlcNAc α2,6 sialyltransferase in adult kidney and also in embryonic and postnatal kidneys. However, it may not be appropriate to relate results of the localization at the cellular level to those obtained from homogenates of the entire organ. We consider it unlikely that the undetectability of α2,3-linked

sialic acids in S1 and S2 segments of proximal tubules and principal cells of collecting ducts is due to a shift from sialylation to fucosylation as reported for postnatal small intestine (Taatjes and Roth 1990), because fucose residues in adult kidney are detectable only in endothelia (Holthöfer et al. 1981; Roth 1983). Based on the lectin blot analysis, we also consider it unlikely that lack of acceptor substrate for the Gal β1,4 GlcNAc α2,3 sialyltransferase, which has been shown in another system to be the rate limiting step (Baum et al. 1996), is the cause although this would require the application of techniques providing higher resolution.

In summary, we found that commonly occurring α2,6- and α2,3-linked sialic acids are differently expressed in the two embryonic anlagen of kidney, exhibit a dynamic expression pattern during nephron morphogenesis and differentiation, and show regional as well as cell type-specific expression in adult kidney.

Acknowledgements We are grateful to U. Schaub for skilled technical assistance, N. Wey for help in preparing the photographs, S. Sulzer for compiling Fig. 14, and A. Schumacher for preparing the manuscript. We would like to thank Dr. B. Kaissling (Institute of Anatomy, University of Zurich) for helpful comments and discussion. This work was supported by the Canton of Zurich and NIH grant GM29470 (to I.J.G.).

References

Al-Awqati Q (1996) Plasticity in epithelial polarity of renal intercalated cells: targeting of the H+-ATPase and band 3. Am J Physiol Cell Physiol 39:C1571–C1580

Al-Awqati Q (2003) Terminal differentiation of intercalated cells: the role of hensin. Annu Rev Physiol 65:567–583

Armstrong JF, Pritchard J-K, Bickmore WA, Hastie ND, Bard JB (1993) The expression of the Wilms' tumour gene, *WT1*, in the developing mammalian embryo. Mech Dev 40:85–97

Bard JB, McConnell JE, Davies JA (1994) Towards a genetic basis for kidney development. Mech Dev 48:3–11

Baum LG, Derbin K, Perillo NL, Wu T, Pang M, Uittenbogaart C (1996) Characterization of terminal sialic acid linkages on human thymocytes: correlation between lectin-binding phenotype and sialyltransferase expression. J Biol Chem 271:10793–10799

Birchmeier C, Birchmeier W (1993) Molecular aspects of mesenchymal–epithelial interactions. Annu Rev Cell Biol 9:511–540

Brown D, Roth J, Orci L (1985) Lectin-gold cytochemistry reveals intercalated cell heterogeneity along rat kidney collecting ducts. Am J Physiol 248:C348–C356

Burger PC, Lotscher M, Streiff M, Kleene R, Kaissling B, Berger EG (1998) Immunocytochemical localization of alpha 2,3(N)-sialyltransferase (ST3Gal III) in cell lines and rat kidney tissue sections: evidence for Golgi and post-Golgi localization. Glycobiology 8:245–257

Charest PM, Roth J (1985) Localization of sialic acid in kidney glomeruli: regionalization in the podocyte plasma membrane and loss in experimental nephrosis. Proc Natl Acad Sci U S A 82:8508–8512

Christensen E, Nielsen S, Moestrup S, Borre C, Maunsbach A, Deheer E, Ronco P, Hammond T, Verroust P (1995) Segmental distribution of the endocytosis receptor gp330 in renal proximal tubules. Eur J Cell Biol 66:349–364

Farquhar MG, Saito A, Kerjaschki D, Orlando RA (1995) The Heymann nephritis antigenic complex: megalin (gp330) and RAP. J Am Soc Nephrol 6:35–47

Gillespie W, Paulson JC, Kelm S, Pang M, Baum LG (1993) Regulation of alpha 2,3-sialyltransferase expression correlates with conversion of peanut agglutinin (PNA)+ to PNA– phenotype in developing thymocytes. J Biol Chem 268:3801–3804

Hammerman M, Rogers S, Ryan G (1992) Growth factors and metanephrogenesis. Am J Physiol 262:F523–F532

Hennet T, Chui D, Paulson JC, Marth JD (1998) Immune regulation by the ST6Gal sialyltransferase. Proc Natl Acad Sci U S A 95:4504–4509

Hilfer SR, Hilfer ES (1983) Computer simulation of organogenesis: an approach to the analysis of shape changes in epithelial organs. Dev Biol 97:444–453

Holthöfer H, Virtanen I (1987) Glycosylation of developing human glomeruli: lectin binding sites during cell induction and maturation. J Histochem Cytochem 35:33–37

Holthöfer H, Virtaanen I, Pettersson E, Törnroth T, Alfthan O, Linder E, Miettinen A (1981) Lectins as fluorescence microscopic markers for saccharides in human kidney. Lab Invest 45:391–399

Horster M, Braun G, Huber S (1999) Embryonic renal epithelia: induction, nephrogenesis, and cell differentiation. Physiol Rev 79:1157–1191

Kaissling B, Dorup J (1995) Functional anatomy of the kidney. In: Greger RF, Knauf H, Mutschler E (eds) Diuretics. Springer, Berlin Heidelberg New York, pp 1–66

Kaneko Y, Yamamoto H, Colley KJ, Moskal JR (1995) Expression of Ga1 beta 1,4GlcNAc alpha 2,6-sialyltransferase and alpha 2,6-linked sialoglycoconjugates in normal human and rat tissues. J Histochem Cytochem 43:945–954

Kelm S, Schauer R (1997) Sialic acids in molecular and cellular interactions. In: Jeon KW (ed) International review of cytology. Academic, San Diego, pp 137–240

Kerjaschki D, Farquhar MG (1982) The pathogenic antigen of Heymann nephritis is a membrane glycoprotein of the renal proximal tubule brush border. Proc Natl Acad Sci U S A 79:5557–5561

Kerjaschki D, Sharky DJ, Farquhar MG (1984) Identification and characterization of podocalyxin: the major sialoprotein of the renal glomerular epithelial cell. J Cell Biol 98:1591–1596

Kiremidjian L, Kopac MJ (1972) Changes in cell adhesiveness associated with the development of *Rana pipiens* pronephros. Dev Biol 27:116–130

Kispert A, Vainio S, McMahon AP (1998) Wnt-4 is a mesenchymal signal for epithelial transformation of metanephric mesenchyme in the developing kidney. Development 125:4225–4234

Knibbs RN, Goldstein IJ, Ratcliffe RM, Shibuya N (1991) Characterization of the carbohydrate binding specificity of the leukoagglutinating lectin from *Maackia amurensis*: comparison with other sialic acid-specific lectins. J Biol Chem 266:83–88

Kreidberg JA, Sariola H, Loring JM, Maeda M, Pelletier J, Housman D, Jaenisch R (1993) WT-1 is required for early kidney development. Cell 74:679–691

Kriz A, Kaissling B (2000) Structural organization of the mammalian kidney. In: Seldin D, Giebisch G (eds) The kidney: physiology and pathophysiology. Raven, New York, pp 587–654

Kumar A, Wallner EI, Carone FA, Scarpelli DG, Kanwar YS (1997) Relevance of proto-oncogenes as growth modulators in organogenesis of the mammalian embryonic kidney. Int J Dev Biol 41:643–653

Kunz A, Brown D, Orci L (1984) Appearance of *Helix pomatia* lectin-binding sites at podocyte plasma membrane during glomerular differentiation: a quantitative analysis using the lectin-gold technique. Lab Invest 51:317–324

Lackie PM, Zuber C, Roth J (1990) Polysialic acid and N-CAM expression in embryonic rat kidney: mesenchymal and epithelial elements show different patterns of expression. Development 110:933–947

Laitinen L, Virtanen I, Saxén L (1987) Changes in the glycosylation pattern during embryonic development of mouse kidney

as revealed with lectin conjugates. J Histochem Cytochem 35:55–65
LeHir M, Dubach UC (1982) The cellular specificity of lectin binding in the kidney. I. A light microscopical study in the rat. Histochemistry 74:521–530
LeHir M, Kaissling B, Koeppen BM, Wade JB (1982) Binding of peanut lectin to specific epithelial cell types in the kidney. Am J Physiol 242:C117–C129
Martin LT, Marth JD, Varki A, Varki NM (2002) Genetically altered mice with different sialyltransferase deficiencies show tissue-specific alterations in sialylation and sialic acid 9-*O*-acetylation. J Biol Chem 277:32930–32938
Matsui K, Breitender-Geleff S, Soleiman A, Kowalski H, Kerjaschki D (1999) Podoplanin, a novel 43-kDa membrane protein, controls the shape of podocytes. Nephrol Dial Transplant 14(suppl 1):9–11
Mo HQ, Winter HC, Goldstein IJ (2000) Purification and characterization of a Neu5Ac alpha 2–6Gal beta 1–4Glc/GlcNAc-specific lectin from the fruiting body of the polypore mushroom *Polyporus squamosus*. J Biol Chem 275:10623–10629
Morelle W, Haslam SM, Ziak M, Roth J, Morris HR, Dell A (2000) Characterization of the *N*-linked oligosaccharides of megalin (Gp330) from rat kidney. Glycobiology 10:295–304
Parr B, McMahon A (1994) *Wnt* genes and vertebrate development. Curr Opin Genet Dev 4:523–528
Paulson JC, Colley KJ (1989) Glycosyltransferases. Structure, localization, and control of cell type-specific glycosylation. J Biol Chem 264: 17615–17618
Pavenstädt H, Kriz W, Kretzler M (2003) Cell biology of the glomerular podocyte. Physiol Rev 83:253–307
Priatel JJ, Chui D, Hiraoka N, Simmons CJT, Richardson KB, Page DM, Fukuda M, Varki NM, Marth JD (2000) The ST3Gal-I sialyltransferase controls CD8(+) T lymphocyte homeostasis by modulating *O*-glycan biosynthesis. Immunity 12:273–283
Rauscher F (1993) The *WT1* Wilms tumor gene product: a developmentally regulated transcription factor in the kidney that functions as a tumor suppressor. FASEB J 7:896–903
Reid PE, Culling CFA, Dunn WL, Clay G, Ramey CE (1978) A correlative chemical and histochemical study of the *O*-acetylated sialic acids of human colonic epithelial glycoproteins in formalin-fixed paraffin-embedded tissues. J Histochem Cytochem 26:1033–1041
Rosenberg A (1995) Biology of the sialic acids. Plenum, New York
Roth J (1983) Application of immunocolloids in light microscopy. II. Demonstration of lectin binding sites in paraffin sections by the use of lectin–gold complexes or glycoprotein–gold complexes. J Histochem Cytochem 31:547–552
Roth J (1989) Postembedding labeling on Lowicryl K4 M tissue sections: detection and modification of cellular components. In: Tartakoff AM (ed) Vesicular transport, methods in cell biology, vol 31. Academic, London, pp 513–551
Roth J, Taatjes D (1985) Glycocalyx heterogeneity of rat kidney urinary tubule: demonstration with a lectin–gold technique specific for sialic acid. Eur J Cell Biol 39:449–457
Roth J, Brown D, Orci L (1983) Regional distribution of *N*-acetyl-D-galactosamine residues in the glycocalyx of glomerular podocytes. J Cell Biol 96:1189–1196
Roth J, Taatjes D, Bitter-Suermann D, Finne J (1987) Polysialic acid units are spatially and temporally expressed in developing postnatal rat kidney. Proc Natl Acad Sci U S A 84:1969–1973
Roth J, Saremaslani P, Zuber C (1992) Versatility of anti-horseradish peroxidase antibody–gold complexes for cytochemistry and in situ hybridization: preparation and application of soluble complexes with streptavidin-peroxidase conjugates and biotinylated antibodies. Histochemistry 98:229–236
Roth J, Zuber C, Sata T, Li W-P (1998) Lectin–gold histochemistry on paraffin and Lowicryl K4 M sections using biotin and digoxigenin-conjugated lectins. In: Rhodes JM, Milton JD (eds) Methods in molecular biology series. Humana, Totowa, NJ, pp 41–53
Sata T, Lackie PM, Taatjes DJ, Peumans W, Roth J (1989) Detection of the NeuAc (α2,3) Gal (β1,4) GlcNAc sequence with the leukoagglutinin from *Maackia amurensis*: light and electron microscopic demonstration of differential tissue expression of terminal sialic acid in α2,3 and α2,6-linkage. J Histochem Cytochem 37:1577–1588
Sata T, Zuber C, Roth J (1990) Lectin-digoxigenin conjugates: a new hapten system for glycoconjugate cytochemistry. Histochemistry 94:1–11
Saxén L (1987) Organogenesis of the kidney. Cambridge University Press, Cambridge
Shibuya N, Goldstein IJ, Broekaert WF, Nsimba-Lubaki M, Peeters B, Peumans WJ (1987) The elderberry (*Sambucus nigra* L.) bark lectin recognizes the Neu5Ac(α2,6)Gal/GalNAc sequence. J Biol Chem 262:1596–1601
Stark K, Vainio S, Vassileva G, McMahon AP (1994) Epithelial transformation of metanephric mesenchyme in the developing kidney regulated by *Wnt-4*. Nature 372:679–683
Taatjes DJ, Roth J (1990) Selective loss of sialic acid from rat small intestinal epithelial cells during postnatal development: demonstration with lectin–gold techniques. Eur J Cell Biol 53:255–266
Taatjes DJ, Roth J, Peumans W, Goldstein IJ (1988) Elderberry bark lectin–gold techniques for the detection of Neu5Ac(α2,6)Gal/GalNAc sequences: applications and limitations. Histochem J 20:478–490
Thiery J, Duband J, Rutishauser U, Edelman G (1982) Cell adhesion molecules in early chicken embryogenesis. Proc Natl Acad Sci U S A 79:6737–6741
Toma V, Zuber C, Sata T, Roth J (1999) Cytochemistry reveals specialized expression of simple *O*-glycans in rat kidney. Glycobiology 9:1191–1197
Toma V, Zuber C, Sata T, Komminoth P, Hailemariam S, Eble JN, Heitz PU, Roth J (2000) Thomsen-Friedenreich glycotope is expressed in developing and normal kidney but not in renal neoplasms. Hum Pathol 31:647–655
Toma V, Zuber C, Winter HC, Goldstein IJ, Roth J (2001) Application of a lectin from the mushroom *Polyporus squamosus* for the histochemical detection of the NeuAc alpha 2,6Gal beta 1,4Glc/GlcNAc sequence of *N*-linked oligosaccharides: a comparison with the *Sambucus nigra* lectin. Histochemistry Cell Biol 116:183–193
Wagner P, Roth J (1988) Occurrence and distribution of sialic acid residues in developing rat glomerulus: investigations with the *Limax flavus* and wheat germ agglutinin. Eur J Cell Biol 47:259–269
Wang WC, Cummings RD (1988) The immobilized leukoagglutinin from the seeds of *Maackia amurensis* binds with high affinity to complex-type asn-linked oligosaccharides containing terminal sialic acid linked α2,3 to penultimate galactose residues. J Biol Chem 263:4576–4585
Weinstein J, de Souza-e-Silva U, Paulson JC (1982) Purification of a Gal beta 1 to 4GlcNAc alpha 2 to 6 sialyltransferase and a Gal beta 1 to 3(4)GlcNAc alpha 2 to 3 sialyltransferase to homogeneity from rat liver. J Biol Chem 257:13835–13844
Zhang B, Palcic MM, Mo H, Goldstein IJ, Hindsgaul O (2001) Rapid determination of the binding affinity and specificity of the mushroom *Polyporus squamosus* lectin using frontal affinity chromatography coupled to electrospray mass spectrometry. Glycobiology 11:141–147
Ziak M, Roth J (1999) Expression of oligo/polyα2,8-linked deaminoneuraminic acid and megalin during kidney development and maturation: mutually exclusive distribution with polyα2,8-linked *N*-acetylneuraminic acid of *N*-CAM. Histochem Cell Biol 112:169–178
Ziak M, Kerjaschki D, Farquhar MG, Roth J (1999) Identification of megalin as the sole rat kidney sialoglycoprotein containing poly alpha 2,8 deaminoneuraminic acid. J Am Soc Nephrol 10:203–209
Zuber C, Li W-P, Roth J (1998) Blot analysis with lectins for the evaluation of glycoproteins in cultured cells and tissues. In: Rhodes JM, Milton JD (eds) Methods in molecular biology series. Humana, Totowa, NJ, pp 159–166